Reflection-asymmetric structures in ^{225}Ra from γ-ray spectroscopy study of ^{229}Th α decay

J. Gasparro, G. Ardisson, and V. Barci
Laboratoire de Radiochimie et Radioécologie, Université de Nice, F-06108 Nice Cédex 2, France

R. K. Sheline
Departments of Chemistry and Physics, Florida State University, Tallahassee, Florida 32306

(Received 11 May 2000; published 9 November 2000)

The level structure of ^{225}Ra, produced in α decay of ^{229}Th, was studied by γ-ray spectroscopy. The sources were continuously purified from daughters with ion-exchange chromatographic separation methods. Energies and intensities of 174 γ rays were accurately measured with HPGe detectors. About 100 γ rays were reported for the first time, especially in the 300–700 keV energy range. A ^{225}Ra level scheme was proposed, accounting for about 200 transitions among 45 excited states. The level structure was interpreted in the framework of reflection-asymmetric structures with parity doublet bands. The model was shown to be in satisfactory agreement with experimental data.

PACS number(s): 21.10.−k, 21.60.Ev, 82.55.+e

I. INTRODUCTION

The study of the nucleus ^{225}Ra is interesting essentially for two reasons: this mass region shows transitions from spherical to deformed shapes and octupole deformations are likely to occur. The existence of stable reflection-asymmetric shapes in atomic nuclei with $A\sim220$ was suggested by potential energy calculations versus octupole deformation [1]. The barrier height between the mirror minima in the potential energy of the quadrupole-octupole surface determines the stability of the asymmetric-deformed nuclear system. For the ^{225}Ra isotope this barrier height was found $\sim$0.8 MeV. Moreover, it was already noted that the measured $1/2^+$ [2] ground-state (g.s.) spin and parity of ^{225}Ra could not be easily explained, unless by introducing an octupole deformation.

Many theoretical approaches were carried out in the past years for odd A nuclei in the mass range $\sim219-229$. Some models considered adiabatic strong coupling of single particle orbitals to a deformed asymmetric core (or mean field) in a folded Yukawa potential [1], or nonadiabatic coupling in deformed Woods-Saxon [3] or Nilsson potential [4]. Dynamic octupole deformations involving a symmetric core coupled to asymmetric/anharmonic phonons [5] were also considered. The deformation parameters were assumed fixed for the whole nucleus [3] or the parameter set was minimized for each configuration [6]. In this latter approach the potential barrier height for the g.s. configuration of ^{225}Ra was found of the same order (0.8 MeV) (as reported also by Briançon *et al.* [7]) as in the previous older calculation [1]. Davydov-Chaban model calculations [8] were also carried out. For other theoretical discussions on the subject see also Refs. [9–12].

Available experimental data on the ^{225}Ra nucleus were reviewed in the compilation paper of Akovali (Ref. [13], and references therein). We ought to mention the ^{225}Fr β decay [14–16] and the neutron transfer reactions ^{226}Ra(d,t) [14] and ^{226}Ra$(^3$He$,\alpha)$ [17] measurements. The γ-ray spectrum from experimental alpha decay of ^{229}Th was extensively studied by Dickens and McConnel [18], Ratan *et al.* [19], and Helmer *et al.* [20,21] with sources in equilibrium mixture with daughters, and high-resolution γ-ray singles, and coincidence measurements. As discussed in Ref. [22] the use of a ^{229}Th source in equilibrium and partially contaminated by ^{228}Th leads to significant Compton background, mainly coming from high-energy γ-ray lines belonging to decay products ($^{208-209}$Tl, ^{212}Bi, ...) towards the end of the chains, so that weak transitions in ^{225}Ra could be masked. We have carried out our measurements with continuous on-line separation and removal of daughters. A preliminary incomplete list of these results, focused on high-energy γ-ray transitions, has been recently published [23]. In this paper we present a review of our experimental methods (Sec. II), a list of γ-ray transitions and a revised level scheme of ^{225}Ra (Sec. III), and a comparison with predictions of asymmetric models (Sec. IV).

II. EXPERIMENTAL METHODS

A. Preparation of the ^{229}Th parent source

A ^{233}U sample of 100-mg weight, unprocessed during the last 20 years, was loaded in 10 M HCl onto a Dowex® 1-X8 anionic column. Uranium isotopes (233 and traces of 232) were fixed as chlorocomplexes, while thorium isotopes (229 and 228) and their daughters passed through. The eluate was evaporated to dryness, brought to 8 M in HNO_3, and loaded onto a column ($\emptyset=10$ mm, $L=200$ mm) filled with Dowex® 1-X4 ion exchanger, previously treated by 8 M HNO_3. The column was washed with 40 cm^3 (eight column volumes) of 8 M HNO_3 to discard all divalent and univalent cations (^{224}Ra, ^{225}Ra, ^{212}Pb, ^{221}Fr) as well as trivalent cations (^{225}Ac), while thorium isotopes (^{229}Th and ^{228}Th) remained fixed at the top as nitratocomplexes $[Th(NO_3)_6]^{2-}$. Bismuth isotopes were also fixed on the resin as nitratocomplexes, but since they have relatively short half-lives (^{212}Bi, $T_{1/2}=60.5$ min; ^{213}Bi, $T_{1/2}=46$ min), we started the counting 2 h after the first elution. Thorium was eluted by 10 M HCl, evaporated to dryness, and dissolved in 1 cm^3 of 8 M HNO_3. This purified solution was loaded on a Dowex® 1-X4 microcolumn ($\emptyset=3$ mm, $L=7$ cm) pretreated with 8 M HNO_3. The

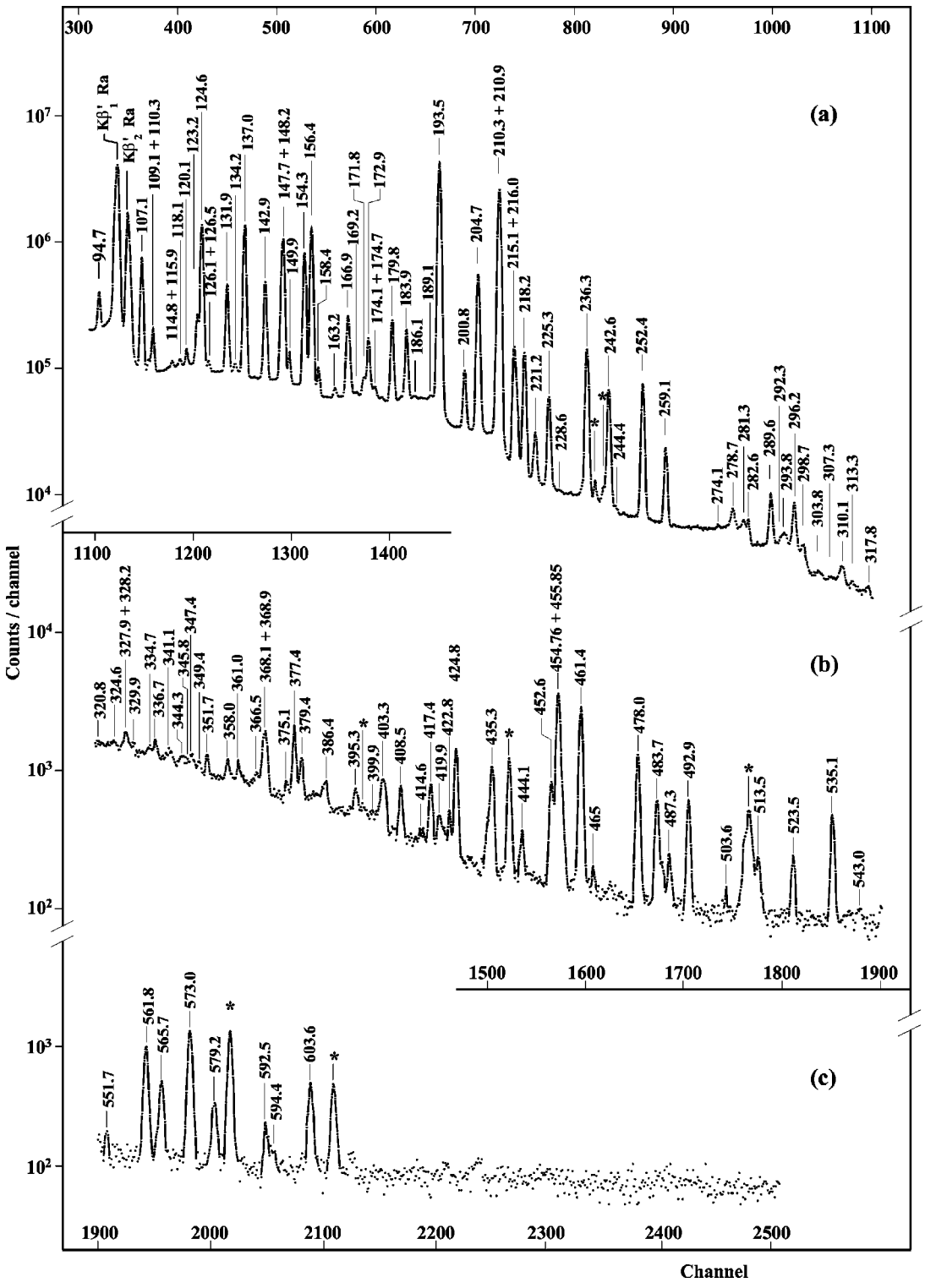

FIG. 1. γ-ray spectrum of ^{229}Th measured with the coaxial detector on the Dowex® 1-X4 column with elution of daughter products. Energies, given in keV, are rounded. Spurious transitions are marked with a star. The energy dispersion is 0.287 keV/channel. (a) $E_\gamma = 90-320$ keV. (b) $E_\gamma = 320-550$ keV. (c) $E_\gamma = 550-880$ keV.

column head, where thorium ions had been fixed, was placed in front of the HPGe detector, at a distance of 3 to 5 cm, and the lower part was shielded with an 1-mm thick lead tube. The top of the column was connected by a teflon tube to a microprocessor-controlled peristaltic pump distributing the eluate through the 8 M HNO_3 reservoir. The detector and the elution column were placed into a 5-cm thick lead castle, the inside covered by 2-mm thick copper sheets.

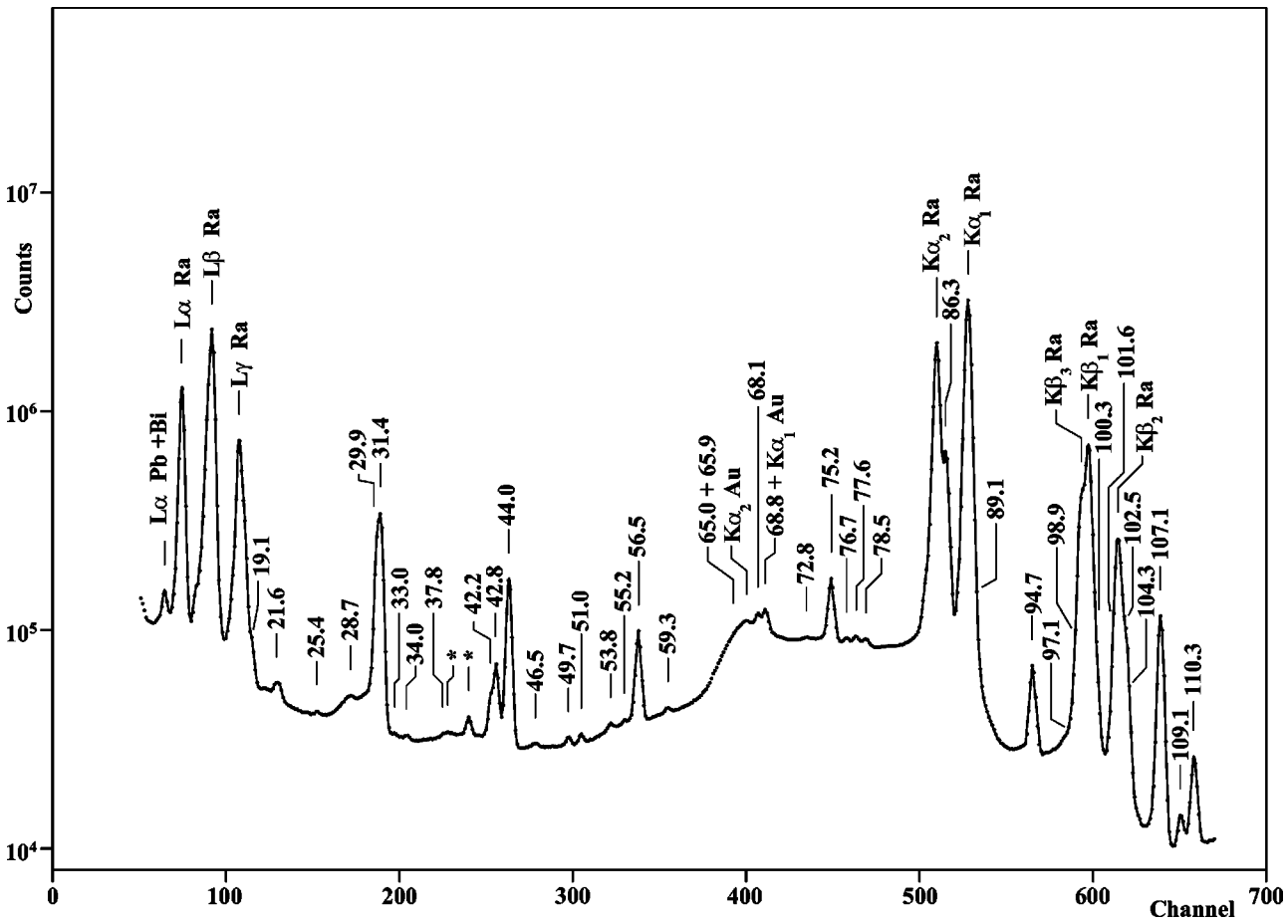

FIG. 2. Part of x-ray and low-energy γ-ray spectrum measured with the planar detector. The energies, rounded, are given in keV. Spurious transitions are marked with a star. The energy dispersion is 0.168 keV/channel.

B. Spectrometers

Two detectors were used to measure the γ-spectra associated with the ^{229}Th α decay. The first was a *p*-type coaxial HPGe detector of 17% relative efficiency, with an energy resolution [full width at half maximum (FWHM)] of 1.9 keV at the 1.33-MeV photopeak of ^{60}Co. The second was a planar [low-energy photon spectrometer (LEPS)] detector of 0.2-cm^3 active volume, with an energy resolution (FWHM) of 190 eV at the 5.9-keV Fe K_α x-ray line. The detector pulses were coupled through a preamplifier-amplifier chain to 8K-channel analyzers (EG&G Ortec). The spectrometers were calibrated in energy and efficiency using standard sources of ^{152}Eu, ^{207}Bi, ^{137}Cs. Several spectra were measured, with different counting times. Figure 1 shows a ^{229}Th γ-ray spectrum measured with the coaxial detector for 23 h and Fig. 2 part of a low-energy x-ray and γ-ray spectrum measured with the LEPS detector for 10 h. Decontamination factors better than 300 were reached for daughter impurities; they were measured by comparing the experimental intensity of the 40.09-keV transition in ^{225}Ra$\rightarrow^{225}$Ac β decay to the equilibrium intensity. Residual background lines present in the spectra come from ^{228}Th decay chain only.

C. Analysis

The analyses of γ-ray spectra were performed with the computer code GAMANAL [24]. Nuclear calculations were carried out with the program package of the ENSDF (Evaluated Nuclear Structure Data Files) program library, provided by NNDC (National Nuclear Data Center, Brookhaven).

III. RESULTS

A. γ-ray energies and intensities

Energies and intensities of 174 γ-ray transitions were accurately measured. The intensities were normalized with respect of the 193.52-keV transition taken as 4.3 per 100 decay [21]. These values are reported in Table I and compared to those of the aforementioned reference; the agreement between the two sets of measurements is generally good, apart for some low-energy weak transitions. A better normalization could be obtained from the accurate measurement of Ref. [20], 4.41(6)%; so a correction factor 1.026(14) should be applied (this correction is not directly reported in the table for comparison reasons). About 100 γ-ray transitions were observed for the first time, especially in the 300–700 keV energy range.

B. The ^{225}Ra level scheme

The ^{225}Ra level scheme was built using our γ-ray data: the level energies were fitted to the energies of the transitions, assigned according to Ritz's principle and at least three

TABLE I. Energies and intensities of γ-ray transitions following the α decay of ^{229}Th. Uncertainties on the last digits of the values are given in parentheses. Unassigned transitions have blank placements; uncertain placements are in parentheses.

This work		Ref. [21]		Placement	
E_γ (keV)	I_γ [a]	E_γ (keV)	I_γ [a]	Initial level (keV)	Final level (keV)
11.1[b] (1)	12[c] (2)	11.1		111.61	100.53
11.79 (20)	≈0.0005			(604.51	592.79)
17.25 (10)	0.22[d] (10)	17.36 (3)		42.74	25.36
19.08 (20)	0.22 (3)				
21.60 (10)	0.08 (2)	21.58 (2)	0.007 (10)		
[e]		23.6	0.0012 (1)	55.23	31.57
25.42 (10)	0.011[d] (2)	25.39 (2)		25.36	0
		27.50 (2)	0.034 (17)		
28.68 (10)	0.10 (3)	30.3		272.20	243.47
29.9[f] (1)	0.11 (2)		0.038 (13)	179.71	149.90
	≈0.002[d]			149.90	120.27
31.43[f] (10)	0.62[d] (8)	31.10 (5)	0.82 (8)	100.53	69.37
	1.86 (20)	31.50 (5)	1.16 (8)	31.57	0
	0.022[d] (10)	31.57 (9)	0.066 (10)	267.95	236.25
33.04 (20)	≈0.01			292.72	260.18
34.02 (20)	≈0.01				
37.78 (20)	0.0030 (2)	37.8 (1)		69.37	31.57
42.24 (10)	0.077 (8)	42.3 (1)	0.080 (8)	111.61	69.37
42.77 (10)	0.17 (2)	42.82 (5)	0.16 (1)	42.74	0
43.99 (5)	0.67 (7)	43.990 (10)	0.64 (3)	69.37	25.36
46.52 (10)	0.0009 (2)	46.52 (4)	0.020 (2)	267.95	220.62
49.74[f] (10)	≈0.005[d]			(151.59	0)
	0.0107 (17)	49.75 (8)	0.021 (2)	321.83	272.20
50.98 (10)	0.0108 (16)	50.99 (4)	0.017 (4)	120.27	69.37
		53.2 (1)			
53.84 (10)	0.020 (3)	53.75 (20)	0.011 (3)	321.83	267.85
55.20 (10)	0.015 (3)	55.11 (3)	0.0026 (4)	55.23	0
56.52 (5)	0.33 (3)	56.518 (5)	0.28 (2)	236.25	179.72
59.33 (10)	0.012 (2)			179.72	120.27
63.7[g]				243.47	179.71
[e]		63.7 (2)	0.005 (2)	284.33	220.62
64.96 (10)	0.085 (11)			(120.27	55.23)
65.91 (10)	0.157 (17)			292.72	226.94
68.1[e,h] (1)		68.09 (4)	0.067 (10)	179.72	111.61
68.2[g]				390.21	321.83
68.80[f] (10)	0.12 (3)	68.83 (3)	0.133 (13)	111.61	42.74
	≈0.04			220.57	151.59
	≈0.09			248.63	179.72
		68.8		272.20	203.47
72.81 (10)	0.012 (3)	72.739 (10)	0.14 (2)	(394.45	321.83)
75.19[f] (10)	0.52 (5)	75.10 (10)	0.59 (13)	100.53	25.36
	0.002 (1)[i]	75.3 (1)		225.08	149.89
76.67 (20)	0.035 (8)				
77.60 (10)	0.054 (6)	77.63 (5)	0.044 (6)	120.27	42.74
78.53 (10)	0.044 (5)	78.3 (2)	0.008 (2)	321.83	243.47
86.33[f] (4)	0.7 (2)	86.25 (4)	1.3 (1)	111.61	25.36
	3.2[d] (4)	86.40 (5)	2.5 (1)	236.25	149.89
89.09[f] (20)	≈0.14			120.27	31.57
				(309.67	220.57)

TABLE I. (*Continued*).

This work		Ref. [21]		Placement	
E_γ (keV)	I_γ [a]	E_γ keV)	I_γ [a]	Initial level (keV)	Final level (keV)
89.09[f] (20)	≈0.01			349.43	260.18
	≈0.005			416.77	327.71
94.70[f] (10)	0.26 (2)	94.73 (2)	0.26 (2)	149.89	55.23
	0.013 (3)	94.92 (8)	0.013 (3)	120.27	25.36
	0.027 (10)			321.83	226.94
97.01 (12)	0.011 (3)			487.22	390.21
98.86 (10)	0.117 (15)			248.63	149.89
100.8 (2)	0.018 (3)	101.1 (2)	0.018 (3)	321.83	220.62
101.58[f] (10)	0.048 (7)			101.72	0
				394.24	292.72
102.54 (2)	0.156 (19)			(327.71	225.08)
104.32 (10)	0.038 (7)	104.6 (2)	0.009 (3)	284.33	179.72
107.11 (10)	0.85 (8)	107.108 (8)	0.79 (4)	149.89	42.74
109.10 (10)	0.029 (3)	109.2	0.043 (8)	220.62	111.61
110.33[f] (5)	0.121 (12)	110.332 (8)	0.121 (12)	179.72	69.37
	0.009[i] (2)			260.18	149.89
114.75 (10)	0.0147 (22)	115.3 (4)	0.027 (4)	592.79	478.10
115.85[f] (10)	≈0.010[d]			216.28	100.53
	0.010 (3)	115.98 (10)	0.017 (3)	236.25	120.27
118.10[f] (10)	0.007 (3)			149.89	31.57
	0.013 (4)	117.99 (15)	0.013 (4)	267.95	149.89
120.08 (5)	0.034 (4)	119.98 (2)	0.05 (2)	220.62	100.53
123.21 (2)	0.155 (16)	123.193 (13)	0.147 (7)	243.47	120.27
124.58[f] (5)	0.78[d] (6)	124.55 (5)	0.67 (6)	149.89	25.36
	0.66 (6)	124.65 (5)	0.72 (6)	236.25	111.61
126.06 (20)	0.0298 (10)	126.4 (2)	0.02 (1)	151.59	0
126.48[f] (10)	0.014 (4)	126.5 (3)	0.011 (5)	226.94	100.53
	0.009[i] (4)			394.45	267.95
		129.04 (3)	0.016 (10)		
131.89 (5)	0.38 (4)	131.926 (5)	0.327 (12)	243.47	111.61
		132.6 (1)			
134.19[f] (10)	0.0092 (15)			203.47	69.37
	0.006[d] (3)	134.2 (1)	0.012 (3)	284.33	149.89
	0.0014[i] (7)			394.24	260.18
		135.71 (7)			
136.97 (5)	1.21 (12)	136.990 (4)	1.15 (3)	179.72	42.74
137.0 (1)	0.04 (1)			248.63	111.61
139.8[i] (1)	0.0045 (10)	140.3 (2)		260.18	120.27
[e]		142.0 (1)	0.011 (3)	321.83	179.72
142.94 (5)	0.40 (4)	142.962 (5)	0.394 (12)	243.47	100.53
		146.8	0.016 (8)		
147.65 (5)	0.23 (2)	147.64 (5)	0.20 (2)	267.95	120.27
148.15 (5)	0.87 (9)	148.15 (4)	0.86 (6)	179.72	31.57
149.89 (10)	0.053 (6)	150.04 (2)	<0.06	149.89	0
151.6[f] (3)				151.59	0
	≈0.025[b]	151.6 (3)		394.45	243.47
154.34 (5)	0.73 (7)	154.336 (10)	0.75 (2)	179.72	25.36
156.38 (5)	1.16 (11)	156.409 (9)	1.16 (3)	267.95	111.61
158.35 (10)	0.040 (4)	158.42 (12)	0.047 (5)	394.45	236.25
		160.6		272.20	111.61
		161.6 (3)			

TABLE I. (*Continued*).

This work		Ref. [21]		Placement	
E_γ (keV)	I_γ [a]	E_γ (keV)	I_γ [a]	Initial level (keV)	Final level (keV)
163.15 (20)	0.0161 (21)	163.34 (17)	0.020 (7)	390.21	226.94
		165.7 (3)			
166.92 (5)	0.222 (22)	166.976 (7)	0.200 (10)	236.25	69.37
167.49 (10)	0.04 (1)	167.45 (5)	0.05 (1)	267.95	100.53
169.2[f] (3)	0.0010[i] (5)			225.08	55.23
	0.0039 (14)	169.09 (3)		390.21	220.62
	0.0029[i] (14)			394.24	225.08
		171.5 (2)	0.018 (5)		
171.76 (5)	0.039 (4)	171.75 (2)	$<$0.04	272.20	100.53
172.91 (10)	0.123 (12)	172.926 (18)	0.11 (1)	284.33	111.61
174.05[f] (11)	$<$0.002[d]	174.82 (2)	$<$0.03	243.47	69.37
	0.0069[d] (18)			390.21	216.28
	0.0065 (18)	174.22 (11)	0.009 (5)	394.45	220.62
174.7 (2)	0.030 (3)			446.45	272.20
179.76 (5)	0.196 (20)	179.757 (7)	0.192 (15)	179.72	0
182.12 (10)	0.0054 (11)			225.08	42.74
183.0 (1)	0.0069 (12)			403.50	220.62
183.93 (10)	0.147 (15)	183.928 (8)	0.138 (7)	284.33	100.53
185.6[f] (1)	$<$0.002[d]			335.40	149.89
	0.011 (2)			478.10	292.72
186.1 (1)	0.013 (5)			446.45	260.18
189.25 (6)	0.0101 (21)			592.79	403.50
190.63 (20)	0.0098 (20)	190.2 (2)		260.18	69.37
193.52[f] (5)	0.0007[i] (3)			225.08	31.57
	4.3 [j]	193.509 (5)	4.3	236.25	42.74
194.94 (20)	0.0162 (23)	194.3 (3)	0.03 (2)	220.62	25.36
200.80 (10)	0.073 (8)	200.807 (16)	0.067 (3)	243.47	42.74
204.69 (5)	0.57 (4)	204.690 (5)	0.58 (3)	236.25	31.57
210.32 (5)	0.26 (3)	210.15 (8)	0.19 (4)	321.83	111.61
210.89 (3)	2.77 (12)	210.853 (3)	2.7 (3)	236.25	25.36
211.47 (10)	0.044 (12)				
213.48 (5)	0.0085 (16)			535.25	321.83
215.13[f] (10)	0.145 (14)	215.100 (10)	0.134 (10)	284.33	69.37
		215.4			
216.0 (1)	0.052 (6)			327.71	111.61
217.41 (10)	0.0063 (11)			260.18	42.74
218.15 (5)	0.134 (12)	218.154 (17)	0.18 (2)	243.47	25.36
219.8[f] (1)	0.0033 (8)			399.54	179.72
	$<$0.0008			446.45	226.94
221.23 (10)	0.024 (2)	221.22 (5)	0.022 (6)	321.83	100.53
225.26[f] (10)	0.003[i] (1)			225.08	0
	0.061 (6)	225.149 (19)	0.070 (10)	267.95	42.74
228.6 (1)	0.0006 (2)			260.18	31.57
234.8t[f] (1)	0.0008[i] (2)			260.18	25.36
	0.0008 (2)			478.10	243.47
236.29 (5)	0.174 (15)	236.249 (8)	0.170 (9)	236.25	0
242.6 (2)	0.081 (8)	242.269 (14)	0.092 (14)	267.95	25.36
		243.5 (3)			
244.4 (1)	0.00127 (32)			394.24	149.89
250.1 (1)	0.00033 (16)			292.72	42.74
252.44 (5)	0.093 (9)	252.43 (3)	0.093 (12)	321.83	69.37

TABLE I. (*Continued*).

This work		Ref. [21]		Placement	
E_γ (keV)	I_γ [a]	E_γ (keV)	I_γ [a]	Initial level (keV)	Final level (keV)
259.05 (10)	0.023 (5)	259.08 (4)	0.033 (5)	284.33	25.36
		261.0 (5)			
267.4 (1)	0.0008 (3)			292.72	25.36
274.1 (1)	0.0007 (2)			394.45	120.27
276.85 (10)	0.0041 (10)			604.51	327.71
		277.48 (5)			
278.65 (5)	0.0066 (8)			390.21	111.61
281.27 (10)	0.007 (1)			608.93	327.71
282.6 (1)	0.0037 (7)			394.45	111.61
289.62 (5)	0.0146 (17)	289.50 (16)	0.006 (4)	390.21	100.53
292.27 (5)	0.0055 (8)				
		292.91 (12)			
293.78 (10)	0.0064 (8)			394.45	100.53
296.21 (10)	0.0161 (17)	296.2 (2)	0.012 (10)	321.83	25.36
298.72 (12)	0.0068 (8)			478.10	179.72
303.75 (10)	0.0017 (3)			335.40	31.57
307.3 (1)	0.006 (3)			486.83	179.72
310.1 (1)	0.00199 (28)			335.40	25.36
313.3 (1)	0.00036 (11)			663.23	349.43
317.8 (1)	0.00053 (14)			349.43	31.57
320.8 (1)	0.00016 (7)			592.79	272.20
324.6 (1)	0.00042 (13)			394.24	69.37
327.9[f] (1)	0.016 (3)			327.71	0
	$<$0.003			663.23	335.40
328.2 (1)	0.0020 (8)			478.10	149.89
329.9 (2)	0.0006 (2)			399.54	69.37
334.74 (10)	0.00042 (11)			446.45	111.61
336.7[f] (1)	$<$0.0001			486.82	149.89
	0.0080 (1)			604.51	267.95
341.1 (1)	0.0008 (2)			663.23	321.83
344.3[f] (1)	$<$0.0001			399.54	55.23
347.4 (1)	0.0006 (1)			416.77	69.37
349.4[f] (1)	0.0004 (1)			349.43	0
	$<$0.0001			592.79	243.47
351.7 (1)	0.0005 (1)			394.45	42.74
358.0 (1)	0.006(1)			478.10	120.27
361.0 (1)	0.0006 (1)			604.51	243.47
366.5[f] (1)	0.0004 (1)			478.10	111.61
	$<$0.0001			486.82	120.27
368.1 (1)	0.0019 (3)			604.51	236.25
368.9 (1)	0.0019 (3)			394.24	25.36
375.1 (1)	0.0003 (1)			486.82	111.61
377.4 (1)	0.0028 (3)			478.10	100.53
379.4 (1)	0.0013 (2)			604.51	225.08
386.4 (1)	0.0008 (2)			486.82	100.53
395.3 (2)	0.0008 (1)			394.45	0
399.9 (2)	0.00014 (6)			399.54	0
403.3 (1)	0.0018 (2)			403.50	0
408.5 (1)	0.0010 (1)			478.10	69.37
414.61 (10)	0.0003 (1)			535.25	120.27
417.4 (1)	0.0014 (2)			486.82	69.37

TABLE I. (*Continued*).

This work		Ref. [21]		Placement	
E_γ (keV)	I_γ [a]	E_γ (keV)	I_γ [a]	Initial level (keV)	Final level (keV)
419.9 (2)	0.0006 (1)			663.23	243.47
422.8 (1)	0.0005 (1)				
424.8 (1)	0.0032 (3)			604.51	179.72
435.3 (1)	0.0031 (4)			478.10	42.74
444.1 (1)	0.0005 (1)			486.82	42.74
452.6 (1)	0.0017 (2)			478.10	25.36
454.76 (10)	0.0102 (11)			604.51	149.89
455.85 (10)	0.0114 (14)				
459.1 (3)	$\approx$0.001			608.93	149.89
461.4 (1)	0.0076 (8)			486.82	25.36
465 (1)	$\approx$0.0001			535.25	69.37
478.0 (1)	0.0036 (4)			478.10	0
483.7 (1)	0.0018 (2)			663.23	220.57
487.3 (2)	0.0004 (1)			486.82	0
492.9 (1)	0.00148 (16)			604.51	111.61
503.6[f] (1)	0.00012 (5)			535.25	31.57
	$<$0.00005			604.51	100.53
513.5 (2)	0.0007 (2)			663.23	149.89
523.5 (1)	0.0005 (1)			592.79	69.37
535.1 (1)	0.0013 (2)			535.25	0
	$<$0.0002			604.51	69.37
543.0 (3)	$\approx$0.0001			663.23	120.27
549.8 (5)	$\approx$0.0001			592.79	42.74
551.7 (2)	0.00011 (4)			663.23	111.61
561.8 (1)	0.0019 (2)			604.51	42.74
565.7 (3)	0.0009 (1)			608.93	42.74
573.0 (1)	0.0027 (3)			604.51	31.57
579.2 (2)	0.0006 (1)			604.51	25.36
592.5 (1)	0.0003 (1)			592.79	0
594.4 (3)	$\approx$0.0001			663.23	69.37
603.6 (2)	0.0009 (2)				

[a]For absolute intensity per 100 decay multiply by 1.026 ± 0.014.
[b]Unobserved in our γ-ray spectra: under our detection limit, but required from ce measurements [27].
[c]Total $I(\gamma+ce)$ calculated from intensity balance.
[d]Calculated from intensity balance.
[e]Required by coincidence measurements; adopted intensity from Ref. [21].
[f]Multiply placed transition. Only the strongest transition is given, or the intensities are suitably divided.
[g]Expected intraband transition.
[h]Unresolved with the 68.80-keV γ ray.
[i]From ^{225}Fr β decay [14].
[j]Normalization transition.

cross-difference agreements. The criterion is evidently necessary but not sufficient, so to complete our assignments we also considered the data on γ-γ, α-e^-, and α-γ coincidences [21], the measured α-particle group energies [21,25,26], the data on ^{225}Fr β decay [14,16], and the level information obtained in ^{226}Ra(d,t) [14] and ^{226}Ra$(^3\mathrm{He},\alpha)$ [17] neutron transfer reactions. These data were used as reported by Akovali [13]. We have to note that many transitions are multiply placed: sometimes they could be resolved using the existing data. If this case we have assigned an intensity only to the strongest transition. The ^{225}Ra level scheme proposed is shown in Fig. 3.

C. Spins and parities

The spins and parities of the levels were assigned primarily in a model independent way, allowing only $E1$, $M1$, and $E2$ multipolarities for the observed γ-ray transitions, following the usual selection rules, and according to the measured conversion-electron (ce) coefficients [21,27] if available.

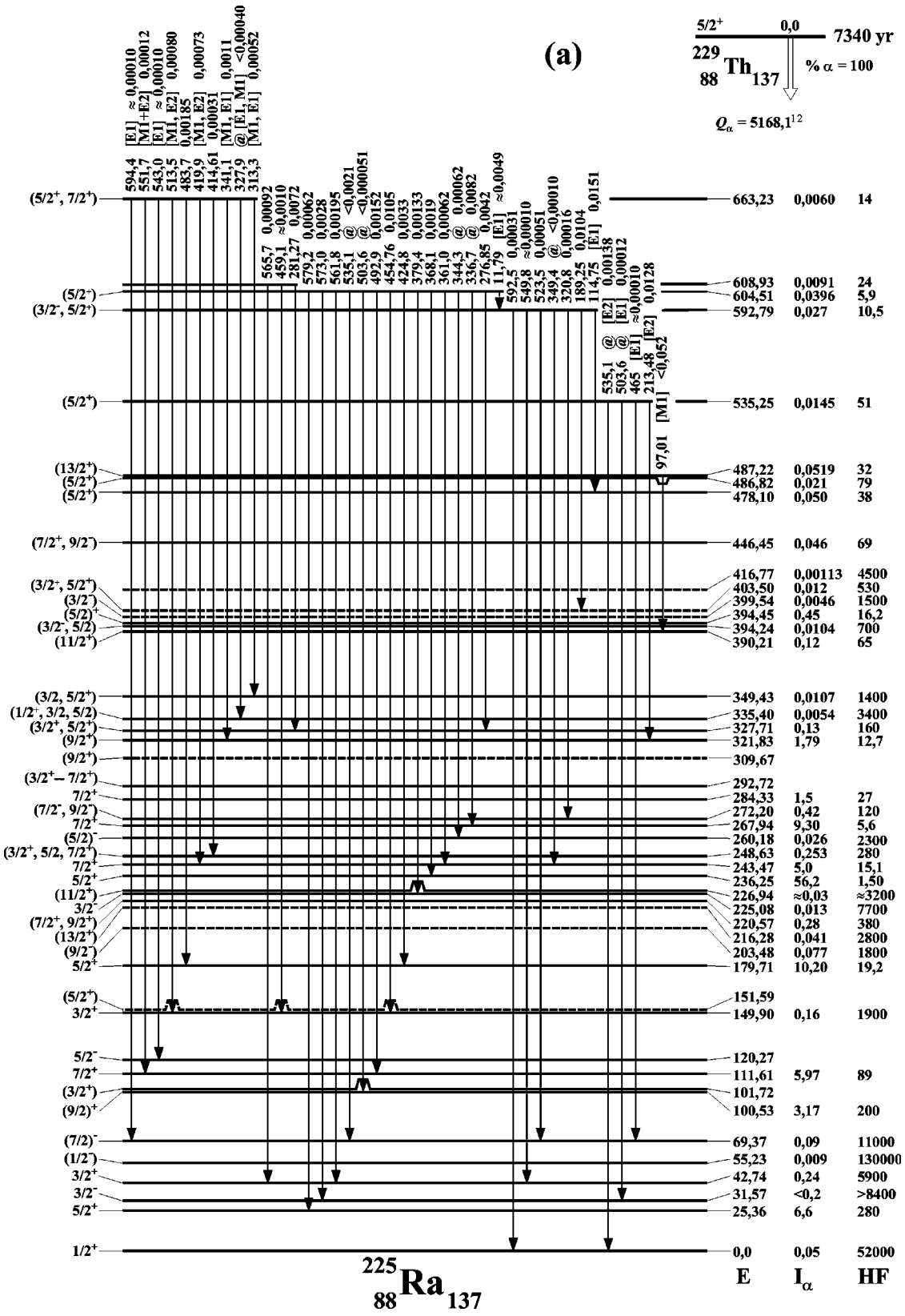

FIG. 3. (a) Level scheme of ^{225}Ra fed in α decay. Energies values in keV are rounded. @ denotes multiply placed γ-ray transitions. Dotted lines are uncertain placements or assignments. Full dots mark known coincidence relations. Multipolarities in square brackets are from level scheme. Total $I(\gamma+ce)$ intensities per 100 decays are given. (b)–(e) (continued).

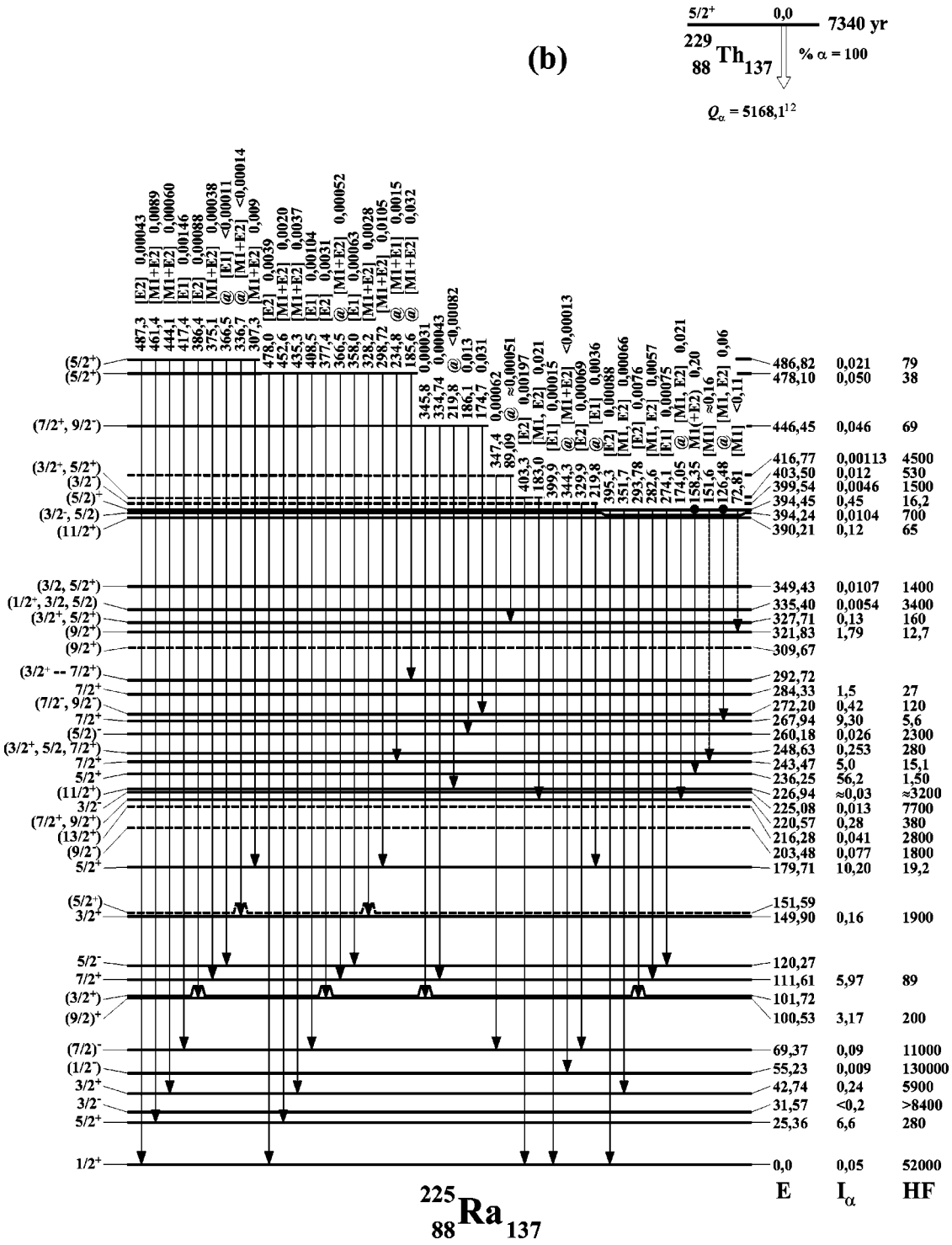

FIG. 3 (*Continued*).

Unambiguous assignments could not be given for some levels, so we quoted ''best'' assignments following theoretical hints as discussed below (Sec. IV). The theoretical calculations are not in contradiction with the experimental data and allow a coherent interpretation of them.

D. Total intensities and α-particle feedings

The α-particle intensities feeding the levels were calculated from the total $(\gamma+ce)$-intensity imbalances at each level. They were found in qualitative agreement with the experimental values from direct α-particle measurements [21,25,26]. In Table II we present the α-particle feedings calculated from total imbalances at each level. We had to note that sometimes the values from γ-ray measurements are less precise than the ones from direct α-particle measurements: the uncertainties come primarily from incomplete knowledge of transition multipolarities. For many of the γ rays we assumed multipolarities allowed by level scheme. In

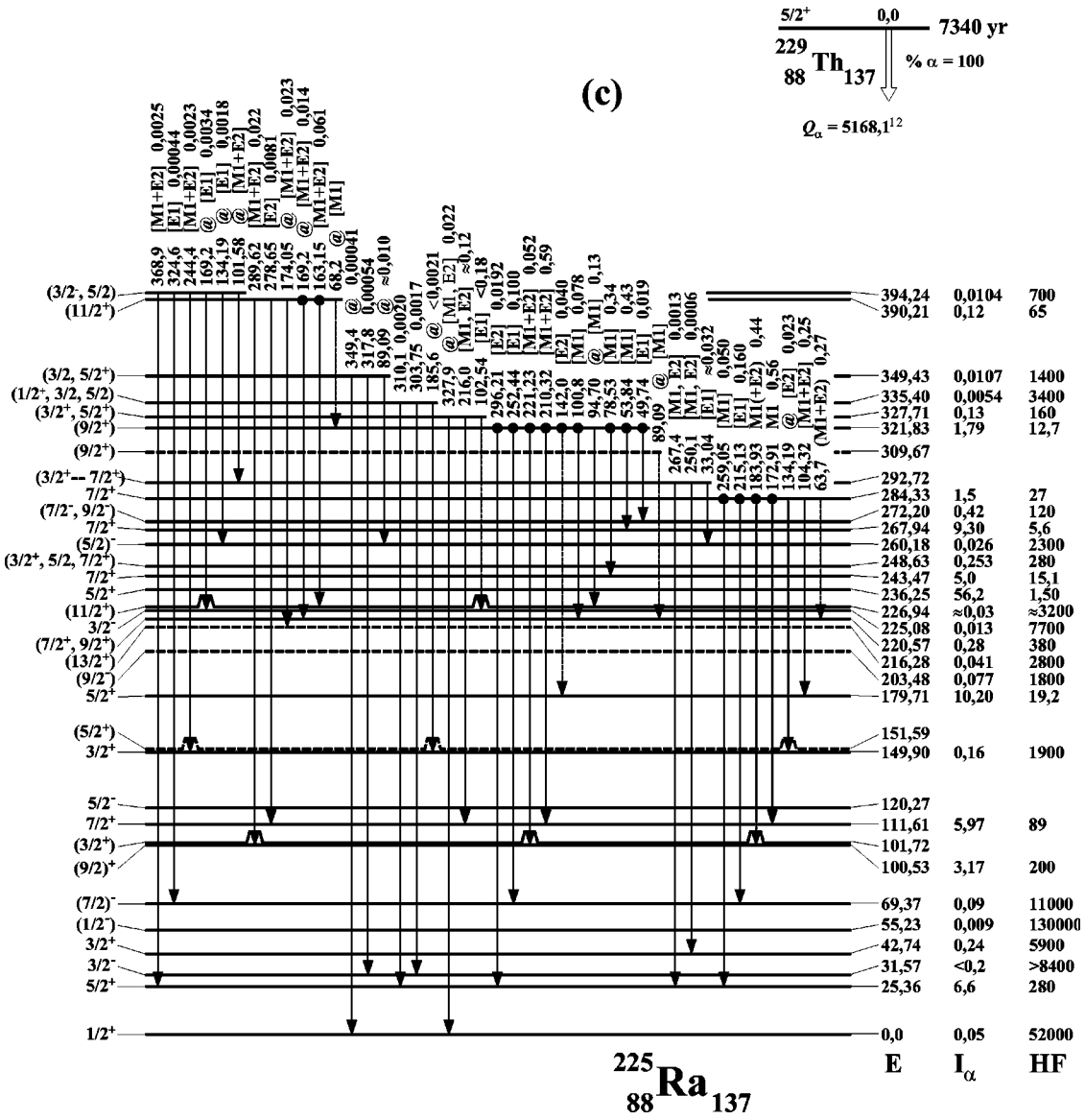

FIG. 3 (*Continued*).

no case these multipolarities were used to establish spins and parities of levels. The values were also reported in Fig. 3. Considering the background in the α-particle spectra of Helmer *et al.* [21] we may estimate a limit of ≈ 0.02 per 100 decays for the intensity of undetected α-particle groups. Weak feedings of this magnitude or lower may have been undetected. Hindrance factors for α-particle branches were calculated according to the adopted α-particle feedings and are also reported in Table II and in Fig. 3.

E. Level discussion

Five excited states proposed in the ^{225}Ra level scheme are new. A further three levels were known only from α-particle measurements with magnetic spectrometry methods of Baranov *et al.* [25,26]; they are now also identified by electromagnetic modes.

We only discuss here some levels with new properties or major changes, with respect to previous data [13,21], and as far as possible in a model independent way. Since the nucleus is relatively well deformed the rotational model could also give some reasonable hints. The $K=1/2^{\pm}$ bands were exhaustively treated by Helmer *et al.* [21]: their assignments are generally confirmed, except in some cases discussed below.

The 101.72-keV level is tentatively identified with the level at 101 keV seen by Nybø *et al.* [14] in (d,t) reaction; their angular distribution favored $I^{\pi}=(3/2^{+})$. The transition to the ground state may be identified as a member of an experimental doublet.

The 203.48-keV level is proposed as the $(9/2^{-})$ member of the $K=1/2^{-}$ band starting at 31.57 keV in place of the 220.54-keV level proposed by Helmer *et al.* [21], as previously suggested by Akovali [13]. This latter level cannot be $I^{\pi}=9/2^{-}$, because of feedings to $5/2^{+}$ and $7/2^{+}$ levels, and from a $7/2^{+}$ level with probable $(M1+E2)$ character. It is appealing to assign this latter state to the same band as the

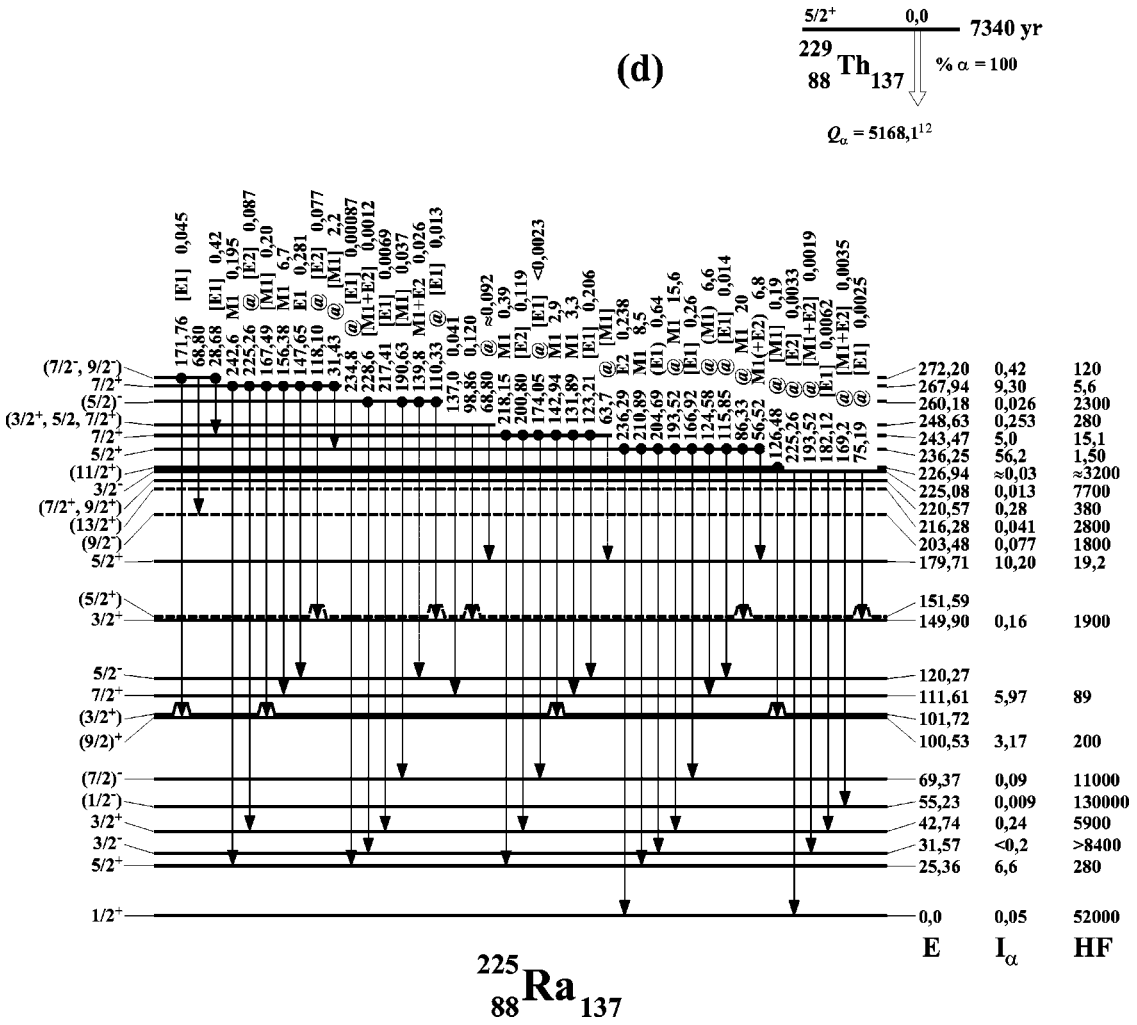

FIG. 3 (*Continued*).

101.72-keV level. Supposing $K=3/2^+$ and $I=7/2^+$ we can calculate $A\approx 9.9$ keV for the inertia parameter of the band, and expect ~ 151 and ~ 310 keV for the $5/2^+$ and $9/2^+$ members. A level at 151.59 keV is possible and allows the placement of the 126.06-keV transition to the 25.37-keV, $5/2^+$, level. Other possible transitions of 151.6 and 49.7 keV may be under our detection limit and/or hidden within an experimental doublet. An intraband transition of 68.8 keV from the 220.55-keV level may also exist, hidden within a multiplet. A highly speculative level $(9/2^+)$ at 309.67 keV could exist, with a weak intraband transition of 89.09 keV, also multiply placed.

The decay modes of the 216.28- and 226.94-keV levels is similar: a single γ-ray to the $(9/2)^+$ state of the g.s. band. Helmer *et al.* [21] proposed the spin and parity $13/2^+$ for the 226.94-keV level and assigned it to the g.s. band. Assigning both to the g.s. band, we propose the spin and parity $11/2^+$ for this level and $13/2^+$ for the 216.28-keV level, similar to the experimental positions of the $5/2^+$ and $9/2^+$ levels, lower than those of the $3/2^+$ and $7/2^+$ levels, respectively.

The 225.08-keV, $3/2^-$, and 260.18-keV, $(5/2^-)$, levels previously known from β decay are also observed in α decay, and identified by their strongest transitions. The weaker ones are not observed, because lower than our detection limit.

A doublet at 394 keV was already known [21]. The 394.24-keV level, seen in β decay only [16], is now observed in α decay also. The 394.45-keV level, observed by Helmer *et al.* [21] on the basis of γ-ray transitions to levels at 220.57 and 267.49 keV, in coincidence with an α-particle group at (4690 ± 2) keV, is confirmed. New transitions of 351.7, 293.78, 282.6, and 274.1 keV may be assigned. A spin and parity of $I^\pi=5/2^+$ are proposed.

A new 403.5-keV state is introduced to place two γ-ray transitions of 403.3 and 183.0 keV to the $1/2^+$ g.s. and the $(7/2^+)$, 220.58-keV level, respectively. The spin and parity should be $I^\pi=(3/2^+, 5/2^+)$.

The 416.77-keV level may correspond to the α-particle group at ~ 4667 keV ($\sim 0.001\%$) [25]. A 347.4-keV transition may be assigned.

The 446.45-keV level may match the (448 ± 4)-keV state observed in the ^{226}Ra(^{3}He,α) reaction [17]. Five transitions can be assigned. From decay modes the allowed spins and parities are $I^\pi=(7/2^+, 9/2^-)$.

The 478.10-keV state matching an α-particle group at (4608 ± 2) keV [21] is firmly established on the basis of 11

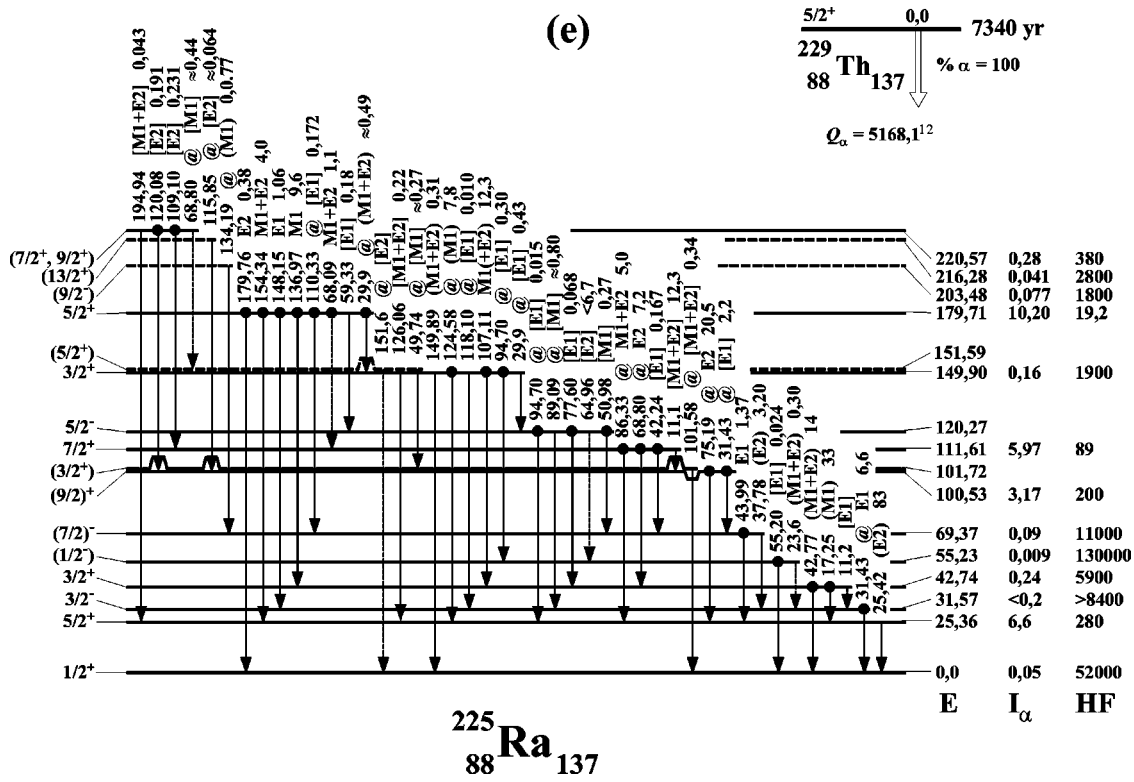

FIG. 3 (*Continued*).

transitions feeding lower excited levels. The most probable spin and parity are $I^{\pi}=(5/2^{+})$. It does not correspond to the 478.4-keV state, previously known from ^{225}Fr β decay [14] and established with coincident transitions, not seen here.

A 486.82-keV level is suggested on the basis of consistent energy-sum relationships; it allows the placement of nine γ-ray transitions. From decay modes its spin and parity may be $I^{\pi}=(5/2^{+})$. This level could be identical with the (484 ± 8)-keV state found in the ^{226}Ra(d,t) reaction, for which Nybø *et al.* [14] suggested a possible doublet structure $I^{\pi}=5/2^{+}$ and $13/2^{+}$. Baranov *et al.* [25,26] also reported a (487 ± 3)-keV level, for which the spin and parity $I^{\pi}=13/2^{+}$ were proposed. Indeed a 97.01-keV transition to the $(11/2^{+})$ level at 390.21 keV could depopulate this state, allowing to place it at 487.22 keV.

A level at 535.29 keV, with spin and parity $I^{\pi}=(5/2^{+})$, is clearly established by six transitions, but it cannot be identified with the (535 ± 8)-keV level observed in neutron transfer reactions [14,17], for which conflicting assignments $(7/2^{+},9/2^{+})$ or $15/2^{-}$ were proposed.

A 592.79-keV level, not detected in α decay [25,21], nor in ^{225}Fr β decay [16], is proposed to place seven new γ-ray transitions. Its spin and parity may be $I^{\pi}=(3/2^{-},\ 5/2^{+})$.

A 603-keV state was earlier proposed by Baranov *et al.* [25,26] to interpret an α-particle group of energy (4484 ± 2) keV. We confirm the existence of this level at 604.51 keV by a lot of new γ rays feeding almost all the low-lying levels. The spin and parity $I^{\pi}=(5/2^{+})$ are the most probable.

The level at 608.93 keV, matching an α-particle group at (4478 ± 3) keV [25] is confirmed by three γ-ray transitions. A new level at 663.23 keV is proposed to place eight γ-ray transitions. Its spin and parity are consistent with $I^{\pi}=(5/2^{+},7/2^{+})$.

IV. DISCUSSION AND COMPARISON WITH THEORY

In Fig. 4 the levels of ^{225}Ra from Fig. 3 are organized so as to emphasize the existence of parity doublet bands as initially suggested in Ref. [1] and analyzed in greater detail in Ref. [4]. Here the band structure and the parity doublet structure are carried somewhat further. This in turn suggests that the nuclear structure we are dealing with in ^{225}Ra involves quadrupole-octupole deformation, either static or dynamic.

In the case of static octupole deformation the coupling between collective octupole modes and the single quasiparticle degrees of freedom is assumed to be strong. The resulting average nuclear field acquires stable reflection-asymmetric deformation, often referred to as strong coupling, by introducing *a priori* a given deformed field with stable octupole deformation. The resulting level diagram is shown in Fig. 5 for single neutron orbitals. It is calculated for an axially symmetric reflection-asymmetric folded Yukawa potential with octupole deformation fixed at $\epsilon_3=0.08$ and is plotted against quadrupole deformation ϵ_2. The orbitals in Fig. 5 are labeled by Ω, and, in parentheses, by the single-particle matrix elements $\langle\hat{s}_z\rangle$, $\langle\hat{\pi}\rangle$ and for $K=1/2$ bands $\langle\hat{\pi}_{\rm conj}|-\hat{J}_{+}|\hat{R}_{\rm conj}\rangle$, corresponding to the decoupling parameter of reflection-symmetric models times parity. Neutron numbers are shown in circles at gaps. Shell model orbitals at $\epsilon_2=\epsilon_3=0$ are also given.

The levels in Fig. 4 are then interpreted for the deformation $\epsilon_2=0.140$ (or $\beta_2=0.148$ in Ref. [3]) in terms of K^{π}

TABLE II. $I_{(\gamma+ce)}$ imbalances compared with I_α's.

E_{level} (keV)	Net feeding				Hindrance factors
	Calculated	Ref. [21]	Ref. [25]	Adopted	
0.0	-4 (16)	0.05 (1)	0.01	0.05	52000
25.36 (3)	2 (22)	6.6 (1)	1.6	6.6 (1)	280
31.57 (4)	0.6 (8)	<0.2	5.2 [a]	<0.2	>8400
42.74 (3)	1 (16)	0.24 (2)	0.24	0.24 (2)	5900
55.23 (7)	0.02 (6)	0.009 (3)		0.009 (3)	130000
69.37 (3)	1.1 (4)	0.09 (1)		0.09 (1)	11000
100.53 (4)	6 (3)	3.4 (1)	3.2	3.17 (4)	200
101.72 (8)	0.08 (16)				
111.61 (3)	5 (4)	7.0 (1)	6.4	5.97[b] (6)	89
120.27 (4)	0.02 (11)				
149.90 (3)	1 (3)	0.21 (2)	0.11	0.16 (5)	1900
151.59 (8)	0.04 (8)				
179.71 (3)	9.8 (23)	10.6 (2)	10.8	10.20 (8)	19.2
203.48 (8)	0.077 (13)		≈ 0.03	0.077 (13)	1800
216.28 (9)	0.041 (11)		≈ 0.03	0.041 (11)	2800
220.57 (5)	0.51 (20)	0.38 (4)	0.18	0.28 (10)	380
225.08 (5)	0.013 (4)			0.013 (4)	7700
226.94 (7)	-0.06 (7)		≈ 0.03	≈ 0.03	≈ 3200
236.56 (3)	56 (4)	53.0	56.2	56.2 (2)	1.50
243.47 (3)	6.0 (5)	5.2	4.8	5.0 (2)	15.1
248.63 (6)	0.253 (19)		≈ 0.29	0.253 (19)	280
260.18 (4)	0.026 (15)			0.026 (15)	2300
267.94 (4)	9.3 (13)	9.6 (2)	8.4	9.30 (8)	5.6
272.20 (5)	0.42 (13)		≈ 0.22	0.42 (13)	120
284.33 (5)	1.8 (3)	1.70 (5)	1.27	1.5 (2)	27
292.69 (6)	0.002 (14)				
321.83 (4)	1.79 (25)	1.40 (4)	0.63	1.79 (25)	12.7
327.71 (4)	0.13 (4)		≈ 0.05	0.13 (4)	160
335.40 (6)	0.0054 (5)		≈ 0.005	0.0054 (5)	3400
349.43 (7)	0.0107 (3)		≈ 0.01	0.0107 (3)	1400
390.21 (5)	0.08 (3)	0.14 (2)	≈ 0.08	0.12 (3)	65
394.24 (6)	0.0104 (22)			0.0104 (22)	700
394.45 (5)	0.45 (6)	0.31 (2)	0.15	0.45 (6)	16.2
399.54 (7)	0.0046 (10)			0.0046 (10)	1500
403.50 (6)	0.012 (9)			0.012 (9)	530
416.76 (10)	0.00113 (11)		≈ 0.001	0.00113 (11)	4500
446.45 (6)	0.046 (6)			0.046 (6)	69
478.10 (4)	0.046 (15)	0.050 (8)		0.050 (8)	38
486.82 (5)	0.021 (5)			0.021 (5)	79
487.22 (13)	0.0519 (14)	0.029 (5)	≈ 0.007	0.0519 (14)	32
535.24 (5)	0.0145 (25)			0.0145 (25)	51
592.79 (5)	0.027 (4)			0.027 (4)	10.5
604.51 (4)	0.0396 (18)	0.050 (7)	≈ 0.009	0.0396 (18)	5.9
608.93 (11)	0.0091 (11)		≈ 0.005	0.0091 (11)	24
663.23 (6)	0.0060 (6)			0.0060 (6)	14

[a]Not observed in Ref. [21].
[b]From Ref. [13].

$=1/2^{\pm}$, $3/2^{\pm}$, $5/2^{\pm}$, and $7/2^{\pm}$ parity doublet bands. This interpretation follows directly from the level structure of Fig. 5. A direct calculation of the effective quadrupole deformation, according to the rotational model formula for the reduced $E2$ transition probability, from the experimental half-life (0.88 ns) of the $5/2^{+}$, 25.36-kev level [28] deexciting to the g.s., gives $\epsilon_2=(0.177\pm0.005)$, and is strictly comparable with the effective deformations of the even-even neighboring nuclei ^{224}Ra ($\epsilon_2=0.169$) and ^{226}Ra ($\epsilon_2=0.191$). (In Ref. [3] the parameter β_2 is used instead of the Nilsson's ϵ_2;

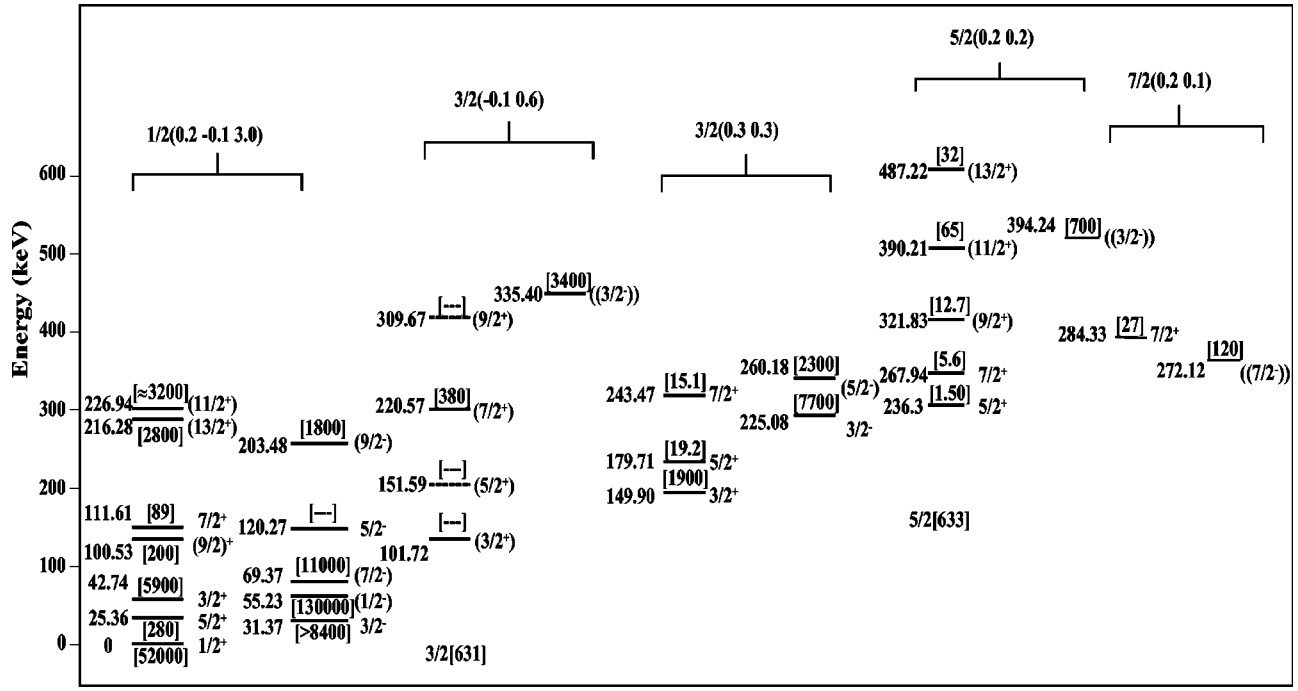

FIG. 4. ^{225}Ra energy levels from Fig. 3, organized into parity doublet bands. The quadrupole-octupole configurations indicated by brackets above the appropriate sets of parity doublet bands are taken from Fig. 5. Some Nilsson's configurations discussed in the text are indicated below the bands.

the usual conversion relation $\epsilon_2 \approx \frac{3}{4}\sqrt{(5/\pi)}\beta_2 = 0.946\beta_2$ holds [29]. The relations between the model parameters, describing the deformed potential, and the effective ones are rather cumbersome [see formulas (2.26)–(2.28) of Ref. [3]]: effective deformations are larger.)

The ground state of ^{225}Ra, with 137 neutrons, is expected (Fig. 5) to give the observed parity doublet $K^\pi = 1/2^\pm$ arising from the configuration 1/2(0.2 −0.1 3.0). Additional excited bands are suggested: the hole configurations 3/2(−0.1 0.6) and 5/2(0.2 0.2) giving rise to $K^\pi = 3/2^\pm$ and $5/2^\pm$ bands and the particle configurations 7/2(0.2 0.1), 3/2(0.2 −0.2), and 5/2(−0.2 0.7) to bands $7/2^\pm$, $3/2^\pm$, and $5/2^\pm$.

The $K^\pi = 1/2^+$ band may be identified up to the $I^\pi = 13/2^+$ state. A two parameter fit gives $A = 5.2$ keV and $a = 1.3$ for inertia and decoupling factor [root mean square (rms) deviation = 4.1 keV]. The $K^\pi = 1/2^-$ partner band is observed up to the member $I^\pi = 9/2^-$; this latter state is not the 220.57-keV level [21], but the 203.48-keV level. This band has fitted parameters $A = 4.6$ keV and $a = -2.5$ (rms = 5.4 keV); the fitted energy splitting of the two bands is 36.8 keV. For a strictly reflection-asymmetric nucleus the parity times decoupling factor values should be equal. The agreement is rather good.

A $K^\pi = 3/2^+$ band, starting at 149.90 keV and with three identified levels, with $A = 4.0$ keV and a $K^\pi = 3/2^-$ band, starting at 225.08 keV, with two levels, and $A = 3.5$ keV, are assigned to the same parity doublet. As is shown by their similar and relatively low inertia parameters they have large deformations ($\epsilon_2 \approx 0.18$), so they must be assigned to the 3/2(0.3 0.3) configuration on the right side of Fig. 5.

The $5/2^+$ band, starting at 236.25 keV, with $A = 5.8$ keV, is strongly populated in α decay with low hindrance factors. Therefore it has been suggested that it must share the same configuration structure as the g.s. of the parent nucleus ^{229}Th, which is known to be a normal quadrupole-deformed configuration $5/2^+[633]$, with $A = 6.1$ keV. The $K^\pi = 5/2^-$ partner is probably very weakly mixed and may be tentatively identified with the band starting with the level at 394.24 keV, which may be $(5/2^-)$, and has a large energy splitting. The corresponding asymmetric configuration is 5/2(0.2 0.2).

The tentative band heads at 284.33 keV, $7/2^+$, and at 272.12 keV, $7/2^-$, may correspond to the configuration 7/2(0.2 0.1). Their very low splitting of energy is the signature of a large parity mixing.

It is interesting to see if the band starting with the state $3/2^+$ at 101.72 keV we proposed in Sec. III may be accounted for by a configuration of Fig. 5. We have shown that the quadrupole deformation ϵ_2 should be low (≈ 0.08) since $A = 9.9$ keV; their shape trends towards a spherical and less deformed configuration and may well be the 3/2[631] Nilsson configuration arising from the $i_{11/2}$ shell of the spherical model, which approaches the Fermi level at low deformation. In this case the asymmetric structure could be the 3/2(−0.1 0.6) configuration. The negative parity partner must be weakly coupled and strongly split: maybe the tentative band starting with the level at 335.40 keV, possibly $3/2^-$, could be the negative partner.

As already noticed by Helmer *et al.* [21] strong Coriolis mixing exists between $\Delta K = 1$ bands in ^{225}Ra. Hindrance factors of α-particle transitions to positive parity levels with $I \geqslant 5/2$ are lower, especially in the $K = 3/2^+$ band starting at 149.90 keV. This is a clear sign of a significant component of the $5/2^+[633]$ configuration in these states. In the experi-

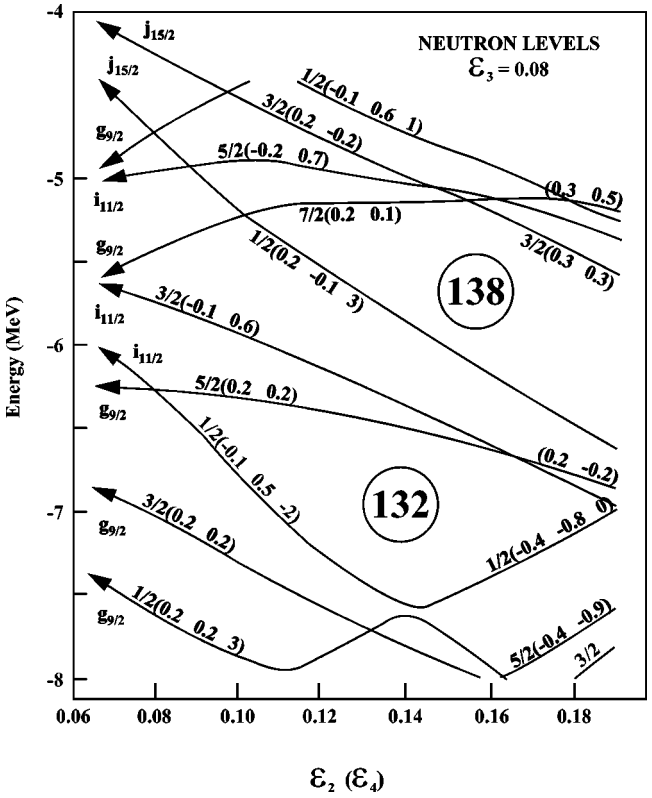

FIG. 5. Single neutron orbitals in an axially symmetric but reflection-asymmetric folded Yukawa potential with $\epsilon_3 = 0.08$ plotted against the quadrupole deformation (ϵ_2). ϵ_4 is a single valued function of ϵ_2. The orbitals are labeled by Ω and in parentheses by a set of single particle matrix elements (see text). Neutron numbers are indicated in circles.

mental level scheme α-particle transitions to positive parity states are generally less hindered than those to negative parity states, in contradiction with the predictions of the asymmetric models, maybe because the core component in the ground state of the parent ^{229}Th is mostly a $K^\pi = 0^+$ reflection-symmetric configuration. A significant exception is the new $K^\pi = 3/2^+$ band we have proposed, starting at 101.72 keV, whose levels are fed by strongly hindered α-particle transition. It may be the sign that its structure is very different from that of the ^{229}Th g.s. Indeed the 5/2[633] configuration arises from the $g_{9/2}$ shell, as does the 3/2[642] configuration which strongly mixes in the favored $K = 3/2^+$ band, while the unfavored band arises from the $i_{11/2}$ shell.

Another remark could be drawn from Fig. 4: the most symmetric configurations, such as the $K^\pi = 3/2^+$ lower band, mostly 3/2[631], and the $K^\pi = 5/2^+$ band, mostly 5/2[633], are those with the largest energy splittings between opposite parity band heads. For the former the splitting is at least 230 keV, for the latter 158 keV. So the parity mixings are also the lowest.

It is evident that in ^{225}Ra configurations with different shapes coexist. The agreement is clearly better if the deformation parameters are fitted to each configuration. In conclusion, the presence of $K^\pi = 1/2^\pm$, $3/2^\pm$, $5/2^\pm$, and $7/2^\pm$ parity doublet bands is supported and also their energy ordering is predicted with relatively good agreement by the calculations shown in Fig. 5.

V. CONCLUSIONS

The γ spectrum following the ^{229}Th α decay were studied using ion exchange chromatographic methods to continuously purify the source from decay products. This procedure allowed us to remove high-energy emitters. As many as 174 γ rays were observed; about 100 were reported for the first time; they were assigned to about 200 transitions among 45 excited states. The resulting ^{225}Ra level structure was interpreted in terms of a series of parity doublet bands following directly from a strong coupling model involving stable octupole deformation.

ACKNOWLEDGMENTS

It is a pleasure to thank Philippe Abela for technical assistance. One of us (R.K.S.) also thanks the Florida State University for support.

[1] G.A. Leander and R.K. Sheline, Nucl. Phys. **A413**, 375 (1984).
[2] S.A. Ahmad, W. Klempt, R. Neugart, E.W. Otten, K. Wendt, C. Ekstrøm, and the ISOLDE Collaboration, Phys. Lett. **133B**, 47 (1983).
[3] G.A. Leander and Y.S. Chen, Phys. Rev. C **37**, 2744 (1988).
[4] R.K. Sheline, A.K. Jain, K. Jain, and I. Ragnarsson, Phys. Lett. B **219**, 47 (1989).
[5] R. Piepenbring, Z. Phys. A **323**, 341 (1986).
[6] P.A. Butler and W. Nazarewicz, Nucl. Phys. **A535**, 249 (1991).
[7] C. Briançon, S. Cwiok, S.A. Eid, V. Green, W.D. Hamilton, C.F. Liang, and R.J. Walen, J. Phys. G **16**, 1735 (1990).
[8] V.Y. Denisov and A.Y. Dzyublik, Nucl. Phys. **A589**, 17 (1995).
[9] R.R. Chasman, Phys. Lett. **96B**, 7 (1980).
[10] I. Ragnarsson, Phys. Lett. **130B**, 352 (1983).
[11] R. Piepenbring, J. Phys. (France) Lett. **45**, L1023 (1984).
[12] R.R. Chasman, Phys. Lett. B **175**, 254 (1986).
[13] Y.A. Akovali, Nucl. Data Sheets **61**, 623 (1990).
[14] K. Nybø, T.F. Thorsteinsen, G. Løvhøiden, E.R. Flynn, J.A. Cizewski, R.K. Sheline, D. Decman, D.G. Burke, G. Sletten, P. Hill, N. Kaffrell, and G. Nyman, Nucl. Phys. **A408**, 127 (1983).
[15] R.K. Sheline, D. Decman, K. Nybø, T.F. Thorsteinsen, G.L. Løvhøiden, E.R. Flynn, J.A. Cizewski, P.D. Burke, G. Sletten, P. Hill, N.K. Kaffrel, W. Kurcewicz, G. Nyman, and G. Leander, Phys. Lett. **133B**, 13 (1983).
[16] E. Andersen, M.J.G. Borge, D.G. Burke, H. Gietz, P. Hill, N. Kaffrell, W. Kurcewicz, G. Løvhøiden, S. Mattsson, R.A. Naumann, K. Nybø, G. Nyman, T.F. Thorsteinsen, and the ISOLDE Collaboration, Nucl. Phys. **A491**, 290 (1989).
[17] G. Løvhøiden, T.F. Thorsteinsen, K. Nybø, and D.G. Burke, Nucl. Phys. **A452**, 30 (1986).

[18] J.K. Dickens and J.W. McConnel, Radiochem. Radioanal. Lett. **47**, 331 (1981).
[19] S.S. Ratan, A.V. Reddy, V.S. Mallapurkar, R.J. Singh, S. Prakash, and M.V. Ramaniah, Phys. Rev. C **27**, 327 (1983).
[20] R.G. Helmer, C.W. Reich, M.A. Lee, and I. Ahmad, Int. J. Appl. Radiat. Isot. **37**, 139 (1986).
[21] R.G. Helmer, M.A. Lee, C.W. Reich, and I. Ahmad, Nucl. Phys. **A474**, 77 (1987).
[22] G. Ardisson, V. Barci, and O. El-Samad, Phys. Rev. C **57**, 612 (1998).
[23] J. Gasparro, G. Barci-Funel, and G. Ardisson, Radiochim. Acta **83**, 1 (1998).
[24] R. Gunnink and J.B. Nidday, Lawrence Livermore National Laboratory Report No. UCRL-51061, 1971,1972, Vols. I–IV (unpublished).
[25] S.A. Baranov, V.M. Shatinskii, and V.M. Kulatov, Yad. Fiz. **10**, 1110 (1969) [Sov. J. Nucl. Phys. **10**, 632 (1970)].
[26] S.A. Baranov, V.M. Shatinskii, V.M. Kulatov, and Y.F. Rodionov, Yad. Fiz. **11**, 925 (1970) [Sov. J. Nucl. Phys. **11**, 515 (1970)].
[27] E.F. Tretyakov, N.I. Tretyakova, V.F. Konyaev, Y.K. Khrudev, A.C. Beda, G.F. Kartashev, and I.N. Vishnevskii, Bull. Acad. Sci. USSR, Phys. Ser. **34**, 763 (1971).
[28] T. Ishii, I. Ahmad, J.E. Gindler, A.M. Friedman, R.R. Chasman, and S.B. Kaufman, Nucl. Phys. **A444**, 237 (1985).
[29] A. Bohr and B. Mottelson, *Nuclear Structure* (Benjamin, New York, 1975), Vol. 2.